Third Edition

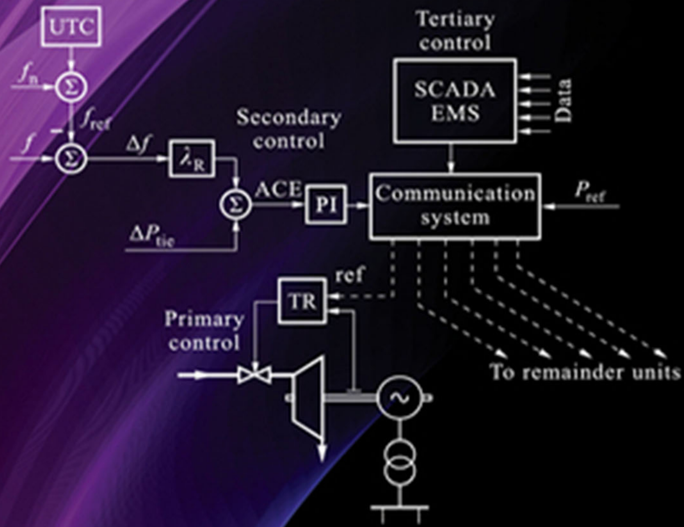

POWER SYSTEM DYNAMICS

STABILITY AND CONTROL

Jan Machowski
Zbigniew Lubosny
Janusz W. Bialek
James R. Bumby

WILEY

Power System Dynamics

Power System Dynamics

Stability and Control

Third Edition

Jan Machowski
Faculty of Electrical Engineering
Warsaw University of Technology
Poland

Zbigniew Lubosny
Faculty of Electrical and Control Engineering
Gdansk University of Technology
Poland

Janusz W. Bialek
formerly Durham University and Edinburgh University
UK

James R. Bumby
formerly Durham University
UK

WILEY

This edition first published 2020

Edition History
Wiley-Blackwell (1e, 2008)
John Wiley & Sons (2e, 2012)

Registered Offices
John Wiley & Sons, Inc., 111 River Street, Hoboken, NJ 07030, USA
John Wiley & Sons Ltd, The Atrium, Southern Gate, Chichester, West Sussex, PO19 8SQ, UK

Editorial Office
The Atrium, Southern Gate, Chichester, West Sussex, PO19 8SQ, UK

For details of our global editorial offices, customer services, and more information about Wiley products visit us at www.wiley.com.

Wiley also publishes its books in a variety of electronic formats and by print-on-demand. Some content that appears in standard print versions of this book may not be available in other formats.

Library of Congress Cataloging-in-Publication Data

Names: Machowski, Jan, author. | Lubosny, Zbigniew, author. |
Bialek, Janusz W., author. | Bumby, James R., author.
Title: Power system dynamics : stability and control /
Jan Machowski, Faculty of Electrical Engineering, Warsaw University of Technology, Poland,
Zbigniew Lubosny, Faculty of Electrical and Control Engineering, Gdansk University of Technology, Poland,
Janusz W. Bialek formerly Durham University and Edinburgh University, UK,
James R. Bumby formerly Durham University, UK.
Description: Third edition. | Hoboken, NJ, USA : John Wiley, 2020. |
Includes bibliographical references and index.
Identifiers: LCCN 2019032080 (print) | LCCN 2019032081 (ebook) |
ISBN 9781119526346 (hardback) | ISBN 9781119526384 (adobe pdf) |
ISBN 9781119526360 (epub)
Subjects: LCSH: Electric power system stability. | Electric power systems–Control.
Classification: LCC TK1010 .M33 2020 (print) | LCC TK1010 (ebook) |
DDC 621.319/1–dc23
LC record available at https://lccn.loc.gov/2019032080
LC ebook record available at https://lccn.loc.gov/2019032081

Cover Design: Wiley
Cover Images: (Power system diagram) courtesy of Jan Machowski, (abstract wave) © oxygen/Getty Images

Set in 9.5/12.5pt STIXTwoText by SPi Global, Pondicherry, India

Printed and bound by CPI Group (UK) Ltd, Croydon, CR0 4YY

10 9 8 7 6 5 4 3 2 1

Contents

About the Authors

Professor Jan Machowski received his MSc and PhD degrees in Electrical Engineering from Warsaw University of Technology in 1974 and 1979, respectively. After obtaining field experience in the Dispatching Center and several power plants, he joined the Electrical Faculty of Warsaw University of Technology, where presently he is employed as a Professor. His areas of interest are electrical power systems, power system protection, and control.

In 1989–1993 Professor Machowski was a Visiting Professor at Kaiserslautern University in Germany, where he carried out two research projects on power swing blocking algorithms for distance protection and the optimal control of FACTS devices.

In 2005–2016 Professor Machowski was Director of Power Engineering Institute at Warsaw University of Technology.

Professor Machowski is the co-author of three books published in Polish: *Power System Stability* (WNT, 1989), *Short Circuits in Power Systems* (WNT, 2008), and *Control of Electric Power Systems* (WPW, 2017). He is also a co-author of *Power System Dynamics and Stability* (John Wiley & Sons, 1997) and *Power System Dynamics: Stability and Control* (John Wiley & Sons, 2008).

Professor Machowski is the author and co-author of over 60 papers published in international fora. He has carried out many projects on electrical power systems, power system stability, and power system protection commissioned by the Polish Power Grid Company, Electric Power Research Institute in the United States, Electroinštitut Milan Vidmar in Slovenia and the Ministry of Science and Education of Poland.

Professor Zbigniew Lubosny received his MSc and PhD degrees in Electrical Engineering from Gdansk University of Technology in 1985 and 1991, respectively, and an MSc in Management also from Gdansk University of Technology in 1987. From 1985 to 2004 he was a lecturer with Gdansk University of Technology. In 2004–2006 he worked at the University of Edinburgh in the UK. In 2006 he again joined Gdansk University of Technology, Faculty of Electrical and Control Engineering, where presently he is employed as a Professor. His areas of interest are electrical power systems, renewable energy systems, and power systems' protection and control.

In 2001 he was EU Marie Curie Individual Fellow in Otto-von-Guericke University Magdeburg in Germany, where he carried out a research project on the influence of renewable energy sources on electric power systems.

Professor Lubosny is the author of a monograph published in English: *Self-organising Controllers of Generating Unit in Electric Power System* (GUT, 1999), the author of a book published in English: *Wind Turbine Operation in Electric Power Systems: Advanced Modeling* (Springer-Verlag, 2003), the author of three books published in Polish: *Wind Turbine Operation in Electric Power Systems* (WNT, 2006), *Wind Farms in the Electric Power System* (WNT, 2009), *Electrical Protection of Wind Farms* (WNT, 2014), and the co-author of a book published in Polish: *Power System Stability* (PWN, 2018).

Professor Lubosny is the author and co-author of over 100 research papers. He has carried out many projects on the protection and control of power systems commissioned by the Polish Power Grid Company, Distribution System Operator Energa SA (EU Horizon 2020 Project), Psymetrix Ltd, UK, the Ministry of Science and Higher Education and other power companies in Poland.

Professor Lubosny is a member of the presidium of the Committee on Electrical Engineering of the Polish Academy of Science, a member of IFAC Power Plants and Power Control Committee, and an editor of the scientific journal *Acta Energetica*.

Professor Janusz W. Bialek received his MEng and PhD degrees in Electrical Engineering from Warsaw University of Technology in 1977 and 1981, respectively. From 1981 to 1989 he was a lecturer at Warsaw University of Technology. After moving to the UK in 1989, he held Chair Professor positions at the University of Edinburgh (2003–2009), Durham University (2009–2014), and since 2019 at Newcastle University. In 2014–2019 he was the Director of Center for Energy Systems at the newly formed Skolkovo Institute of Science and Technology (Skoltech) in Russia. He is a Fellow of the Institute of Electrical and Electronics Engineers (IEEE).

Professor Bialek's main research interest is in the application of advanced mathematical methods to power system analysis. He has published widely on power system dynamics, smart grids, preventing electricity blackouts, power markets, and the technical and economic integration of renewable generation in power systems. He has been the Principal Investigator of a number of major research grants funded by the UK's Engineering and Physical Sciences Research Council (EPSRC) and a consultant to the UK government, International Energy Agency, European Commission, Scottish government, and a number of power companies. Since 2015, he has also been the non-executive independent director of KEGOC (Kazakhstan Electricity Grid Operating Company).

Dr. James R. Bumby received his BSc and PhD degrees in Engineering from Durham University in 1970 and 1974, respectively. From 1973 to 1978 he worked for the International Research and Development Company, Newcastle-upon-Tyne, on superconducting machines, hybrid vehicles, and sea-wave energy. He joined the Engineering Science Department (now School of Engineering) at Durham University in 1978, where he worked as a Lecturer, Senior Lecturer, and Reader in Electrical Engineering until his retirement in 2009. He worked in the general area of electrical machines and systems for over 35 years, first in industry and then in academia.

Dr. Bumby is the author or co-author of over 100 technical papers and three books in the general area of electrical machines and power systems and control. He has also written numerous technical reports for industrial clients. He published his first book, a research monograph, *Superconducting Rotating Electrical Machines* in 1983 (Oxford University Press). He is a co-author of *Power System Dynamics and Stability* (John Wiley & Sons, 1997) and *Power System Dynamics: Stability and Control* (John Wiley & Sons, 2008). These papers and books have led to the award of a number of national and international prizes, including the Institute of Measurement and Control prize for the best transactions paper in 1988 for work on hybrid electric vehicle drive systems and the IEE Power Division Premium in 1997 for work on direct drive permanent magnet generators for wind turbine applications.

List of Symbols & Abbreviations

Notation

Italic type denotes scalar physical quantity (e.g. R, L, C) or numerical variable (e.g. x, y).
Phasor or complex quantity or numerical variable is underlined (e.g. $\underline{I}$, $\underline{V}$, $\underline{S}$).
Italic with arrow on top of a symbol denotes a spatial vector (e.g. $\vec{F}$).
Italic boldface denotes a matrix or a vector (e.g. $\boldsymbol{A}$, $\boldsymbol{B}$, $\boldsymbol{x}$, $\boldsymbol{y}$).
Unit symbols are written using roman type (e.g. Hz, A, kV).
Standard mathematical function are written using roman type (e.g. sin, cos).
Numbers are written using roman type (e.g. 5, 6).
Symbols representing numbers are written using roman type (e.g. π, e = 2.718282 – John Napier number, j – angular shift by 90°, a – angular shift by 120°).
Matrix transposition T is written using roman type.
Differential and partial differential coefficients are written using roman type (e.g. $\frac{\mathrm{d}f}{\mathrm{d}x}, \frac{\partial f}{\partial x}$).
Symbols describing objects are written using roman type (e.g. TRAFO, LINE).
Subscript relating to objects is written using roman type (e.g. $\underline{I}_{\mathrm{TRAFO}}$, $\underline{I}_{\mathrm{LINE}}$).
Subscript relating to physical quantity or numerical variable is written using italic type (e.g. A_{ij}, x_k).
Subscripts A, B, C refer to three-phase axes of a generator.
Subscripts d, q refer to the direct- (d-axis) and quadrature-axis (q-axis) components.
Lower case symbols normally denote instantaneous values (e.g. v, i).
Upper case symbols normally denote RMS or peak values (e.g. V, I).

Symbols

a, a^2	operators shifting the angle by 120° and 240°, respectively.
B_{μ}	magnetizing susceptance of a transformer.
B_{sh}	susceptance of a shunt element.
D	damping coefficient.
E_{k}	kinetic energy of the rotor relative to the synchronous speed.
E_{p}	potential energy of the rotor with respect to the equilibrium point.
e_{f}	field voltage referred to the fictitious q-axis armature coil.
e_{q}	steady-state emf induced in the fictitious q-axis armature coil proportional to the field winding self-flux linkages.
e'_{d}	transient emf induced in the fictitious d-axis armature coil proportional to the flux linkages of the q-axis coil representing the solid steel rotor body (round-rotor generators only).

e'_{q}	transient emf induced in the fictitious q-axis armature coil proportional to the field winding flux linkages.
e''_{d}	subtransient emf induced in the fictitious d-axis armature coil proportional to the total q-axis rotor flux linkages (q-axis damper winding and q-axis solid steel rotor body).
e''_{q}	subtransient emf induced in the fictitious q-axis armature coil proportional to the total d-axis rotor flux linkages (d-axis damper winding and field winding).
$\underline{E}$	steady-state internal emf.
$\underline{E}_{f}$	excitation emf proportional to the excitation voltage V_{f}.
E_{fm}	peak value of the excitation emf.
E_{d}	d-axis component of the steady-state internal emf proportional to the rotor self-linkages due to currents induced in the q-axis solid steel rotor body (round-rotor generators only).
E_{q}	q-axis component of the steady-state internal emf proportional to the field winding self-flux linkages (i.e. proportional to the field current itself).
$\underline{E}'$	transient internal emf proportional to the flux linkages of the field winding and solid steel rotor body (includes armature reaction).
E'_{d}	d-axis component of the transient internal emf proportional to flux linkages in the q-axis solid steel rotor body (round-rotor generators only).
E'_{q}	q-axis component of the transient internal emf proportional to the field winding flux linkages.
$\underline{E}''$	subtransient internal emf proportional to the total rotor flux linkages (includes armature reaction).
E''_{d}	d-axis component of the subtransient internal emf proportional to the total flux linkages in the q-axis damper winding and q-axis solid steel rotor body.
E''_{q}	q-axis component of the subtransient internal emf proportional to the total flux linkages in the d-axis damper winding and the field winding.
$\underline{E}_{r}$	resultant air-gap emf.
E_{rm}	amplitude of the resultant air-gap emf.
$\boldsymbol{E}_{G}$	vector of the generator emf's.
f	mains frequency.
f_{n}	rated frequency.
$\vec{F}$	magnetomotive force (mmf) due to the field winding.
$\vec{F}_{a}$	armature reaction mmf.
$F_{a\ ac}$	ac armature reaction mmf (rotating).
$F_{a\ dc}$	dc armature reaction mmf (stationary).
$\vec{F}_{ad}, \vec{F}_{aq}$	d- and q-axis components of the armature reaction mmf.
$\vec{F}_{f}$	resultant mmf.
G_{Fe}	core loss conductance of a transformer.
G_{sh}	conductance of a shunt element.
H_{ii}, H_{ij}	self and mutual synchronizing power.
i_{A}, i_{B}, i_{C}	instantaneous currents in phases A, B, and C.
$i_{A\ dc}, i_{B\ dc}, i_{C\ dc}$	DC component of the current in phases A, B, and C.
$i_{A\ ac}, i_{B\ ac}, i_{C\ ac}$	ac component of the current in phases A, B, and C.
i_{d}, i_{q}	currents flowing in the fictitious d- and q-axis armature coils.
i_{D}, i_{Q}	instantaneous d- and q-axis damper winding current.
i_{f}	instantaneous field current of a generator.

$\boldsymbol{i}_{\mathrm{ABC}}$	vector of instantaneous phase currents.
$\boldsymbol{i}_{\mathrm{fDQ}}$	vector of instantaneous currents in the field winding and the d- and q-axis damper windings.
$\boldsymbol{i}_{\mathrm{0dq}}$	vector of armature currents in the rotor reference frame.
$\underline{I}$	armature current.
$\underline{I}_{\mathrm{d}}$, $\underline{I}_{\mathrm{q}}$	d- and q-axis component of the armature current.
$\underline{I}_{\mathrm{S}}$, $\underline{I}_{\mathrm{R}}$	currents at the sending and receiving end of a transmission line.
$\underline{\boldsymbol{I}}_{\mathrm{R}}$, $\underline{\boldsymbol{I}}_{\mathrm{E}}$	vector of complex current injections to the retained and eliminated nodes.
$\underline{\boldsymbol{I}}_{\mathrm{G}}$, $\underline{\boldsymbol{I}}_{\mathrm{L}}$	vector of complex generator and load currents.
$\Delta\underline{\boldsymbol{I}}_{\mathrm{L}}$	vector of load corrective complex currents.
J	moment of inertia.
j	operator shifting the angle by 90°.
k_{PV}, k_{QV}	voltage sensitivities of the load (the slopes of the real and reactive power demand characteristics as a function of voltage).
k_{Pf}, k_{Qf}	frequency sensitivities of the load (the slopes of the real and reactive power demand characteristics as a function of frequency).
$K_{E_{\mathrm{q}}}$	steady-state synchronizing power coefficient (the slope of the steady-state power angle curve $P_{E_{\mathrm{q}}}(\delta)$).
$K_{E'_{\mathrm{q}}}$	transient synchronizing power coefficient (the slope of the transient power angle curve $P_{E'_{\mathrm{q}}}(\delta')$).
$K_{E'}$	transient synchronizing power coefficient (the slope of the transient power angle curve $P_{E'}(\delta')$).
K_i	reciprocal of droop for the i-th generating unit.
K_{L}	frequency sensitivity coefficient of the system real power demand.
K_{T}	reciprocal of droop for the total system generation characteristic.
l	length of a transmission line.
L_{AA}, L_{BB}, L_{CC}, L_{ff}, L_{DD}, L_{QQ}	self-inductances of the windings of the phase windings A, B, and C; the field winding; and the d-and the q-axis damper winding.
L_{d}, L_{q}	inductances of the fictitious d- and q-axis armature windings.
L'_{d}, L'_{q}, L''_{d}, L''_{q}	d- and q-axis transient and subtransient inductances.
L_{xy}	where x, y∈{A, B, C, D, Q, f} and x ≠ y are the mutual inductances between the windings denoted by the indices as described above.
L_{S}	minimum value of the self-inductance of a phase winding.
ΔL_{S}	amplitude of the variable part of the self-inductance of a phase winding.
$\boldsymbol{L}_{\mathrm{R}}$	submatrix of the rotor self- and mutual inductances.
$\boldsymbol{L}_{\mathrm{S}}$	submatrix of the stator self- and mutual inductances.
$\boldsymbol{L}_{\mathrm{SR}}$, $\boldsymbol{L}_{\mathrm{RS}}$	submatrices of the stator-to-rotor and rotor-to-stator mutual inductances.
M	coefficient of inertia.
M_{f}, M_{D}, M_{Q}	amplitude of the mutual inductance between a phase winding and, respectively, the field winding and the d- and q-axis damper winding.
N	generally, number of turns of a winding.
p	number of poles.
P, Q	active (real) and reactive power, respectively.
P_{acc}	accelerating power.
P_{D}	damping power.
P_{e}	electromagnetic air-gap power.

$P_{E_\mathrm{q}\ \mathrm{cr}}$ critical (pull-out) air-gap power developed by a generator.

$P_{E_\mathrm{q}}(\delta)$, $P_{E'}(\delta')$, $P_{E'_\mathrm{q}}(\delta')$ air-gap power curves assuming E_q = constant, E' = constant, and E'_q = constant.

P_g in induction machine (Chapter 7), real power supplied from the grid (motoring mode) or supplied to the grid (generating mode).

P_L real power absorbed by a load or total system load.

P_m mechanical power supplied by a prime mover to a generator; also mechanical power supplied by a motor to a load (induction machine in motoring mode, Chapter 7).

P_n real power demand at rated voltage.

P_R real power at the receiving end of a transmission line.

P_rI, P_rII, P_rIII, P_rIV contribution of the generating units remaining in operation toward covering the real power imbalance during the first, second, third, and fourth stage of load frequency control.

P_sI, P_sII, P_sIII, P_sIV contribution of the system toward covering the real power imbalance during the first, second, third, and fourth stage of load frequency control.

P_s stator power of induction machine (Chapter 7).

P_S real power at the sending end of a transmission line or real power supplied by a source to a load or real power supplied to the infinite busbar.

P_SIL surge impedance (natural) load.

$P_{\mathrm{s}E_\mathrm{q}}(\delta)$ curve of real power supplied to the infinite busbar assuming E_q = constant.

P_T total power generated in a system.

P_tie net tie-line interchange power.

$P_{V_\mathrm{g}}(\delta)$ air-gap power curve assuming V_g = constant.

$P_{V_\mathrm{g}\ \mathrm{cr}}$ critical value of $P_{V_\mathrm{g}}(\delta)$.

Q_L reactive power absorbed by a load.

Q_G reactive power generated by a source (the sum of Q_L and the reactive power loss in the network).

Q_n reactive power demand at rated voltage.

Q_R reactive power at the receiving end of a transmission line.

Q_S reactive power at the sending end of a transmission line or reactive power supplied by a source to a load.

R resistance.

r total resistance between (and including) the generator and the infinite busbar.

R_A, R_B, R_C, R_D, R_Q, R_f resistances of the phase windings A, B, and C; the d- and q-axis damper winding; and the field winding.

$\boldsymbol{R}_\mathrm{ABC}$ diagonal matrix of phase winding resistances.

$\boldsymbol{R}_\mathrm{fDQ}$ diagonal matrix of resistances of the field winding and the d- and q-axis damper windings.

s Laplace operator.

s slip of induction motor.

s_cr critical slip of induction motor.

S_n rated apparent power.

S_SHC short-circuit power.

t time.

T'_d, T''_d short-circuit d-axis transient and subtransient time constants.

T'_do, T''_do open-circuit d-axis transient and subtransient time constants.

T'_q, T''_q short-circuit q-axis transient and subtransient time constants.

T'_{qo}, T''_{qo}	open-circuit q-axis transient and subtransient time constants.
T_a	armature winding time constant.
$\boldsymbol{T}$	transformation matrix between network (a, b) and generator (d, q) coordinates.
v_A, v_B, v_C, v_f	instantaneous voltages across phases A, B, and C and the field winding.
v_d, v_q	voltages across the fictitious d- and q-axis armature coils.
v_w	wind speed.
$\boldsymbol{v}_{ABC}$	vector of instantaneous voltages across phases A, B, and C.
$\boldsymbol{v}_{fDQ}$	vector of instantaneous voltages across the field winding and the d- and q-axis damper windings.
V	Lyapunov function.
V_{cr}	critical value of the voltage.
$\underline{V}_d$, $\underline{V}_q$	d- and q-axis component of the generator terminal voltage.
V_f	voltage applied to the field winding.
$\underline{V}_g$	voltage at the generator terminals.
$\underline{V}_s$	infinite busbar voltage.
$\underline{V}_{sd}$, $\underline{V}_{sq}$	d- and q-axis component of the infinite busbar voltage.
$\underline{V}_S$, $\underline{V}_R$	voltage at the sending and receiving end of a transmission line.
V_{sh}	local voltage at the point of installation of a shunt element.
$\underline{V}_i = V_i\angle\delta_i$	complex voltage at node *i*.
$\underline{\boldsymbol{V}}_R$, $\underline{\boldsymbol{V}}_E$	vector of complex voltages at the retained and eliminated nodes.
W	work.
$\boldsymbol{W}$	Park's modified transformation matrix.
$\boldsymbol{W}$, $\boldsymbol{U}$	modal matrices of right and left eigenvectors.
X_a	armature reaction reactance (round-rotor generator).
X_C	reactance of a series compensator.
X_D	reactance corresponding to the flux path around the damper winding.
X_d, X'_d, X''_d	d-axis synchronous, transient, and subtransient reactance.
x_d, x'_d, x''_d	total d-axis synchronous, transient, and subtransient reactance between (and including) the generator and the infinite busbar.
$x'_{d\,PRE}$, $x'_{d\,F}$, $x'_{d\,POST}$	pre-fault, fault, and post-fault value of x'_d.
X_f	reactance corresponding to the flux path around the field winding.
X_l	armature leakage reactance of a generator.
X_q, X'_q, X''_q	q-axis synchronous, transient and subtransient reactance.
x_q, x'_q, x''_q	total q-axis synchronous, transient, and subtransient reactance between (and including) the generator and the infinite busbar.
X_{SHC}	short-circuit reactance of a system as seen from a node.
Y_T	admittance of a transformer.
$\underline{\boldsymbol{Y}}$	admittance matrix.
$\underline{\boldsymbol{Y}}_{GG}$, $\underline{\boldsymbol{Y}}_{LL}$, $\underline{\boldsymbol{Y}}_{LG}$, $\underline{\boldsymbol{Y}}_{LG}$	admittance submatrices, where subscript G corresponds to fictitious generator nodes and subscript L corresponds to all the other nodes (including generator terminal nodes).
$\underline{Y}_{ij} = G_{ij} + jB_{ij}$	element of the admittance matrix.
$\underline{\boldsymbol{Y}}_{RR}$, $\underline{\boldsymbol{Y}}_{EE}$, $\underline{\boldsymbol{Y}}_{RE}$, $\underline{\boldsymbol{Y}}_{ER}$	complex admittance submatrices, where subscript E refers to eliminated and subscript R to retained nodes. $Z = \sqrt{r^2 + x_d x_q}$.
Z_c	characteristic impedance of a transmission line.

$\underline{Z}_{\mathrm{s}} = R_{\mathrm{s}} + \mathrm{j}X_{\mathrm{s}}$	internal impedance of the infinite busbar.
$\underline{Z}_{\mathrm{T}} = R_{\mathrm{T}} + \mathrm{j}X_{\mathrm{T}}$	series impedance of the transformer.
$\Delta\omega$	rotor speed deviation equal to $(\omega - \omega_{\mathrm{s}})$.
γ	instantaneous position of the generator d-axis relative to phase A.
γ_0	position of the generator d-axis at the instant of a fault.
$\varPhi_{\mathrm{a}}$	armature reaction flux.
$\varPhi_{\mathrm{ad}}$, $\varPhi_{\mathrm{aq}}$	d- and q-axis component of the armature reaction flux.
$\varPhi_{\mathrm{a\ ac}}$	ac armature reaction flux (rotating).
$\varPhi_{\mathrm{a\ dc}}$	dc armature reaction flux (stationary).
$\varPhi_{\mathrm{f}}$	excitation (field) flux.
$\varPsi_{\mathrm{A}}$, $\varPsi_{\mathrm{B}}$, $\varPsi_{\mathrm{C}}$	total flux linkage of phases A, B, and C.
$\varPsi_{\mathrm{AA}}$, $\varPsi_{\mathrm{BB}}$, $\varPsi_{\mathrm{CC}}$	self-flux linkage of phases A, B, and C.
$\varPsi_{\mathrm{a\ ac\ r}}$	rotor flux linkages produced by $\varPhi_{\mathrm{a\ ac}}$.
$\varPsi_{\mathrm{a\ dc\ r}}$	rotor flux linkages produced by $\varPhi_{\mathrm{a\ dc}}$.
$\varPsi_{\mathrm{a\ r}}$	rotor flux linkages produced by the total armature reaction flux.
$\varPsi_{\mathrm{D}}$, $\varPsi_{\mathrm{Q}}$	total flux linkage of damper windings in axes d- and q.
$\varPsi_{\mathrm{d}}$, $\varPsi_{\mathrm{q}}$	total d- and q-axis flux linkages.
$\varPsi_{\mathrm{f}}$	total flux linkage of the field winding.
$\varPsi_{\mathrm{fa}}$	excitation flux linkage with armature winding.
$\varPsi_{\mathrm{fA}}$, $\varPsi_{\mathrm{fB}}$, $\varPsi_{\mathrm{fC}}$	excitation flux linkage with phases A, B, and C.
$\boldsymbol{\varPsi}_{\mathrm{ABC}}$	vector of phase flux linkages.
$\boldsymbol{\varPsi}_{\mathrm{fDQ}}$	vector of flux linkages of the field winding and the d- and q-axis damper windings.
$\boldsymbol{\varPsi}_{\mathrm{0dq}}$	vector of armature flux linkages in the rotor reference frame.
τ_{e}	electromagnetic torque.
τ_{m}	mechanical torque.
τ_{ω}	fundamental-frequency subtransient electromagnetic torque.
$\tau_{2\omega}$	double-frequency subtransient electromagnetic torque.
τ_{d}, τ_{q}	d- and q-axis component of the electromagnetic torque.
τ_{R}, τ_{r}	subtransient electromagnetic torque due to stator and rotor resistances.
ε	rotor acceleration.
φ_{g}	power factor angle at the generator terminals.
δ	power (or rotor) angle with respect to the infinite busbar.
δ_{g}	power (or rotor) angle with respect to the voltage at the generator terminals.
$\hat{\delta}_{\mathrm{s}}$	stable equilibrium value of the rotor angle.
δ'	transient power (or rotor) angle between E' and V_{s}.
δ_{fr}	angle between the resultant and field mmf's.
λ_{R}	frequency bias factor.
$\underline{\lambda}_i = \alpha_i + \mathrm{j}\varOmega_i$	eigenvalue.
ω	angular velocity of the generator (in electrical radians).
ω_{s}	synchronous angular velocity in electrical radians (equal to $2\pi f$).
ω_{T}	rotor speed of wind turbine (in rad/s).
$\varOmega$	frequency of rotor swings (in rad/s).
$\boldsymbol{\varOmega}$	rotation matrix.
ρ	static droop of the turbine-governor characteristic.
ρ_{T}	droop of the total system generation characteristic.
ϑ	transformation ratio.

γ	propagation constant of a transmission line.
β	phase constant of a transmission line.
$\Re$	reluctance.
$\Re_d$, $\Re_q$	reluctance along the d- and q-axis.
ζ	damping ratio.

Abbreviations

AC	alternating current
ACE	area control error
AGC	automatic generation control
AGSS	automatic generation shedding scheme
ANN	artificial neural network
AR	autoregressive
ARMAX	autoregressive moving average with exogenous input model
ARX	autoregressive with exogenous input model
AVR	automatic voltage regulator
BESS	battery energy storage system
BFP	breaker failure protection
BIMP	Bureau international des poids et mesures
BTA	balanced truncation approximation
CCGT	combined cycle gas turbine
CCPP	combined-cycle power plant
CCT	critical clearing time
CESA	continental Europe synchronous area
CIM	current injection model
COI	center of inertia
CSC	controlled series capacitor
CT	current transformer
d-axis	direct-axis of a generator
DC	direct current
DFIG	doubly-fed induction generator
DFIM	doubly-fed induction machine
DSA	dynamic security assessment
DSO	distribution system operator
EHV	extra high voltage
emf	electromotive force
EMS	energy management system
ENTSO-E	European Network of Transmission System Operators for Electricity
EPS	electric power system
FACTS	flexible AC transmission system
FC	fixed capacitor
FRC	fully rated converter
FRT	fault ride through

GEP	generator-exciter-power system
GV	governor valves
GPS	global positioning system
GTO	gate turn-off thyristor
HAWT	horizontal-axis wind turbine
HP	high pressure
HRB	heat-recovery boiler
HRSG	heat-recovery steam generator
HV	high voltage
HVDC	high voltage direct current
HVRT	high-voltage ride through
IGBT	insulated gate bipolar transistor
IGCT	integrated gate-commutated thyristor
IGV	inlet guide vanes
Im	imaginary axis
IP	intermediate pressure
IV	intercept valves
K3, K2E, K2, K1	short circuits: three-phase, two-phase-ground, two-phase, single-phase
LFC	load and frequency control
LLFT	lower linear fractional transformation
LP	low pressure
LQE	linear-quadratic estimator
LQI	linear-quadratic-Gaussian regulator with tracking loop based on integral element
LQR	linear-quadratic regulator
LTC	load tap changer
LVRT	low-voltage ride through
MAWS	mean annual wind speed
MIMO	multiple inputs and multiple outputs
mmf	magnetomotive force
MSV	main emergency stop valves
OEL	overexcitation limiter
OLEC	overload emergency state control
OLTC	on-load tap changer
OPF	optimal power flow
OST	out-of-step tripping
PCC	point of common coupling
PCS	power conditioning system
PDC	phasor data concentrator
PMU	phasor measurement unit
POD	power oscillation damper
PSB	power swing blocking
PSD	power swing detection
PSP	pole-slip protection
PSS	power system stabilizer
pu	per unit